**Atmospheric
Chemistry
and Physics**

Modelling of the photooxidation of toluene: conceptual ideas for validating detailed mechanisms

V. Wagner[1], M. E. Jenkin[2], S. M. Saunders[1, *], J. Stanton[1], K. Wirtz[3], and M. J. Pilling[1]

[1]School of Chemistry, University of Leeds, Leeds LS2 9JT, UK
[2]Imperial College, Silwood Park, Ascot, Berkshire SL5 7PY, UK
[3]Centro de Estudios Ambientales del Mediterraneo, C. Charles R. Darwin 14, 46980 Paterna, Spain
[*]present address: School of Earth and Geographical Science, University of Western Australia, 6009, Western Australia

Abstract. Toluene photooxidation is chosen as an example to examine how simulations of smog-chamber experiments can be used to unravel shortcomings in detailed mechanisms and to provide information on complex reaction systems that will be crucial for the design of future validation experiments. The mechanism used in this study is extracted from the Master Chemical Mechanism Version 3 (MCM v3) and has been updated with new modules for cresol and γ-dicarbonyl chemistry. Model simulations are carried out for a toluene-NO_x experiment undertaken at the European Photoreactor (EUPHORE). The comparison of the simulation with the experimental data reveals two fundamental shortcomings in the mechanism: OH production is too low by about 44%, and the ozone concentration at the end of the experiment is over-predicted by 55%. The radical budget was analysed to identify the key intermediates governing the radical transformation in the toluene system. Ring-opening products, particularly conjugated γ-dicarbonyls, were identified as dominant radical sources in the early stages of the experiment. The analysis of the time evolution of radical production points to a missing OH source that peaks when the system reaches highest reactivity. First generation products are also of major importance for the ozone production in the system. The analysis of the radical budget suggests two options to explain the concurrent under-prediction of OH and over-prediction of ozone in the model: (1) missing oxidation processes that produce or regenerate OH without or with little NO to NO_2 conversion or (2) NO_3 chemistry that sequesters reactive nitrogen oxides into stable nitrogen compounds and at the same time produces peroxy radicals. Sensitivity analysis was employed to identify significant contributors to ozone production and it is shown how this technique, in combination with ozone isopleth plots, can be used for the design of validation experiments.

1 Introduction

The photooxidation of aromatic hydrocarbons contributes significantly to the formation of urban photochemical smog. Detailed mechanisms are used to calculate photochemical ozone creation potentials (POCPs) for organic compounds that assist policy makers in defining realistic pollution control strategies (Derwent et al., 1998). Derwent et al. (1996) have shown from trajectory model calculations that about one third of the regional ozone production for a typical air mass in northwest Europe is caused by aromatics. In that study toluene is identified as the VOC with the highest ozone production along the trajectory, owing to a combination of high emissions and a comparatively high POCP value.

The oxidation of toluene proceeds via several channels that result either in ring-retaining or ring-opening products. The two prevailing ring-retaining routes, which form cresol and benzaldehyde as first generation products, are comparatively well understood (Atkinson, 1992; Klotz et al., 1998; Volkamer et al., 2002), whereas the chemistry of the ring-opening routes is still very speculative (Smith et al., 1998; Volkamer et al., 2001; Yu and Jeffries, 1997). Over the past years several ring-opening routes have been proposed in line with emerging experimental information (Atkinson et al., 1980; Bartolotti and Edney, 1995; Klotz et al., 1997).

Correspondence to: M. J. Pilling
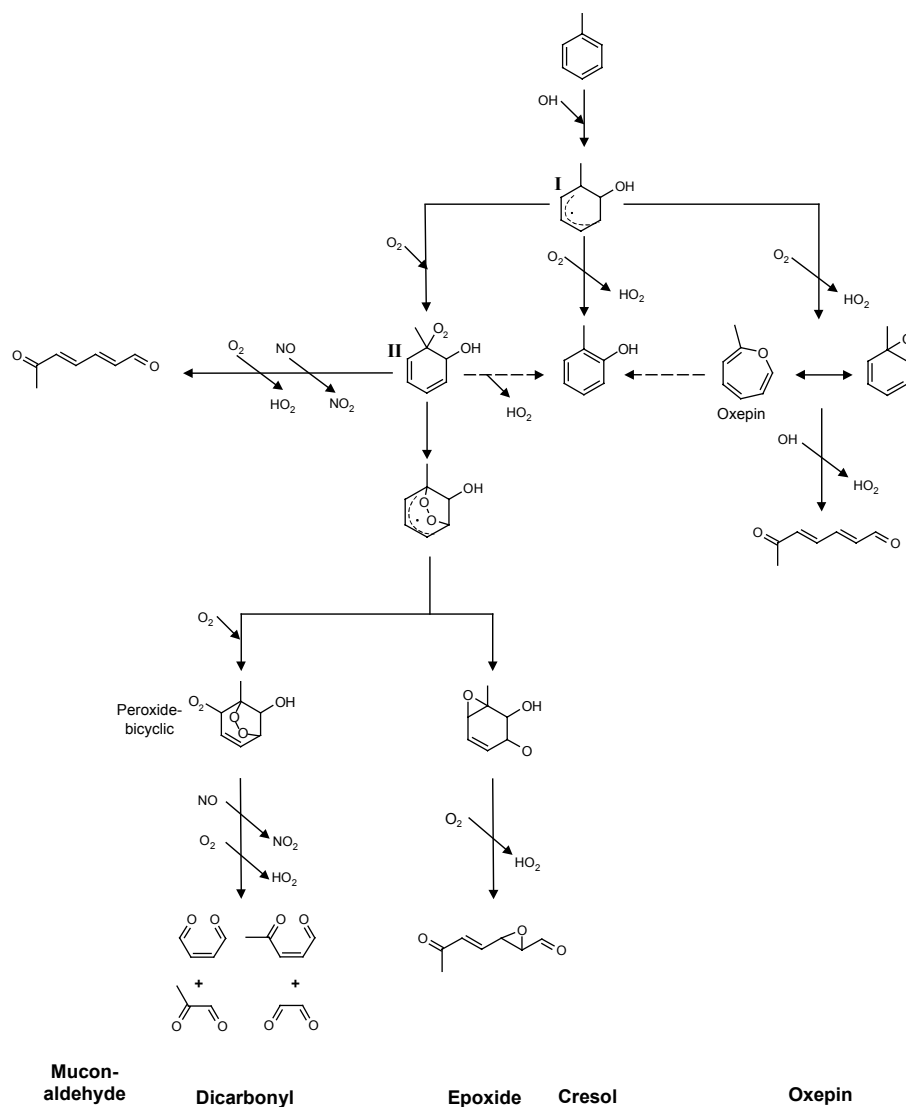(M.J.Pilling@chem.leeds.ac.uk)

Fig. 1. Initial reaction steps of the OH initiated oxidation of toluene as discussed in current literature. Names at the bottom of the figure are labels for the reaction routes as used in this publication. Only major pathways that follow the addition of OH to the ring are considered, the quinone route (1,4 addition of OH and O_2) and the benzaldehyde route (H-abstraction from the methyl group) are not shown. The mechanisms of all routes are still very speculative. From the radical intermediates only the aromatic-OH adduct (I) and the hydroxycyclohexadienyl type peroxy radical (II) have been detected in laboratory experiments. Evidence for the epoxide route is very tentative, and all attempts to detect oxepin in toluene oxidation systems have failed so far. See text for further explanations.

This development, which is reflected in three versions of the MCM, is outlined in the following (Fig. 1 and Fig. 2).

Based on detection of ring-opening products, such as glyoxal and methylglyoxal, Atkinson et al. (1980) proposed a reaction channel (here labelled as dicarbonyl route) in which the ring breaks down via a series of peroxide-bicyclic intermediates eventually forming α-dicarbonyls (glyoxal and methylglyoxal) and conjugated γ-dicarbonyls (butenedial, 2-methylbutenedial and 4-oxo-2-pentenal). In the mid-nineties quantum mechanical calculations published by Bartolotti and Edney (1995) suggested that an epoxide-type compound is

the most stable intermediate following the OH addition to the ring. This result shifted the attention to a reaction pathway (termed hereon as epoxide route) in which epoxides are the dominant reaction products. Following this direction, Yu and Jeffries (1997) were indeed able to find experimental evidence for this route by detecting compounds with molecular weights matching a series of putative epoxide intermediates. A further reaction route was proposed based on observations of prompt HO_2 formation at high yields in the toluene and benzene oxidation system by flash photolysis experiments (Klotz et al., 1997). These high yields of direct HO_2 for-
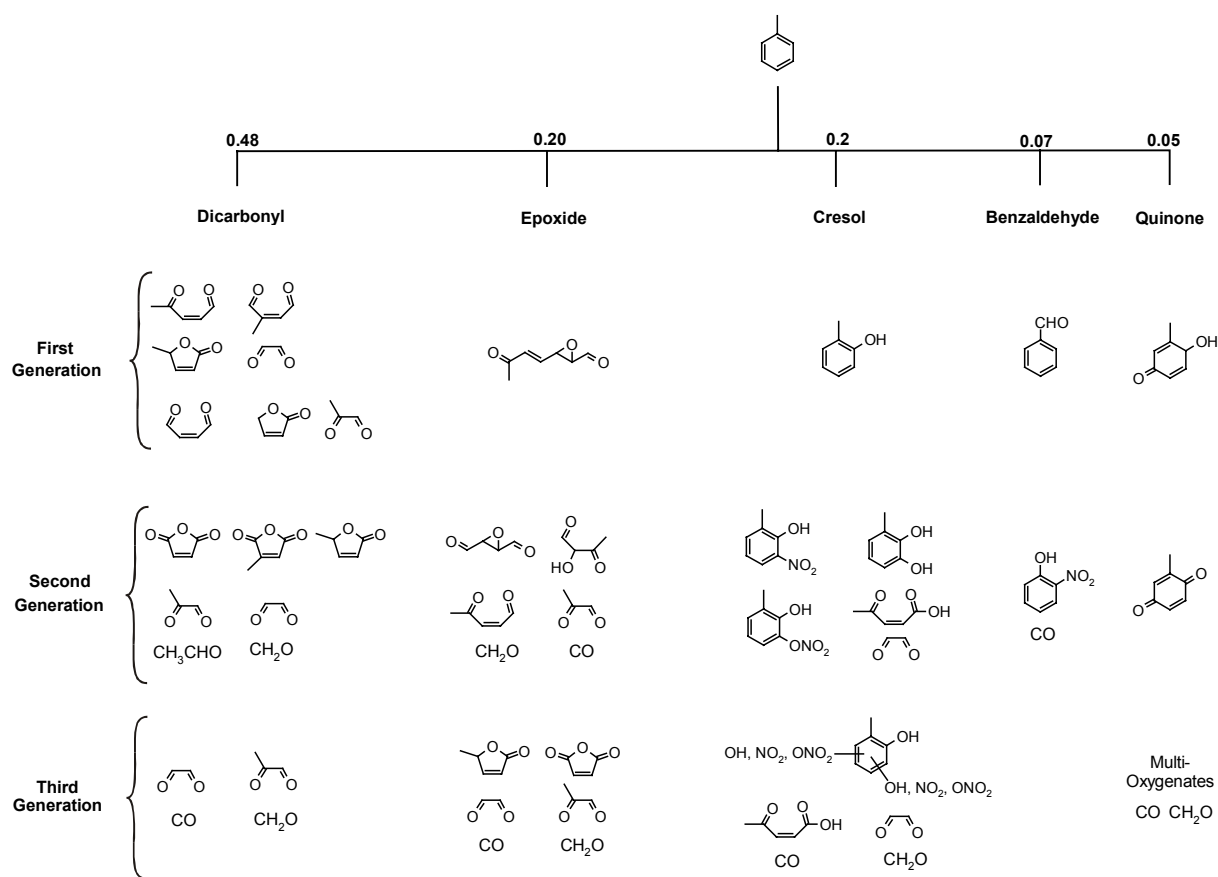
Fig. 2. Major reaction products in the toluene photooxidation system as implemented in the TOL_MCM3a model used in this study (CO_2 is not shown). Note, branching ratios for ring-opening routes are speculative, particularly for the epoxide-route as for this pathway only qualitative evidence exists.

mation, without an NO to NO_2 conversion step, indicated a further reaction channel, in addition to the phenol route, that produces prompt HO_2 (Klotz et al., 2000; Bohn and Zetsch, 1999; Bohn, 2001). Based on these findings Klotz et al. (1997) suggested an aromatic oxide/oxepin route with muconaldehydes as ring-opening products and prompt HO_2 production. The mechanism for this route was developed by analogy with the metabolism of benzene. Berndt et al. (1999) carried out an experimental study to investigate this reaction pathway, but no evidence for the formation of aromatic oxide/oxepin could be found.

Owing to a lack of quantitative information on ring-opening products, branching ratios for the ring-opening pathways have not yet been established. However, most quantitative evidence has been found for intermediates that are consistent with the ring-opening route proposed by Atkinson et al. (1980).

A number of mechanisms have been developed to describe the photooxidation of aromatic compounds (Liang and Jacobson, 2000). They show varying degrees of explicit treatment. With 670 implemented reactions for

the photooxidation of toluene, the MCM v3 aims to reflect the most detailed current knowledge in the field of toluene photo-oxidation (http://www.chem.leeds.ac.uk/Atmospheric/MCM/mcmproj.html). According to the historic development in the field of aromatic photooxidation, the MCM v1, launched in 1997, contained a toluene mechanism based mainly on a ring-opening route as proposed by Atkinson et al. (1980). For MCM v2 a toluene mechanism was developed that explored the proposed degradation route involving the formation of aromatic oxide/oxepin intermediates (Klotz et al., 2000). Subsequently, as no evidence could be found for significant contribution from the aromatic oxide/oxepin route (Berndt et al., 1999), this channel has been replaced in the MCM v3 by dicarbonyl and epoxide routes.

In comparisons with smog-chamber data, the MCM v1 toluene mechanism over-predicts $[O_3]$ by a factor of around 2 (Liang and Jacobson, 2000). The MCM v2, on the other hand, shows too little photochemical reactivity and under-predicts O_3 formation significantly if compared to toluene smog-chamber experiments (this study, unpublished results). The MCM v3 predicts time-concentration profiles for NO_x

($NO_x = NO + NO_2$), O_3 and toluene that are in comparatively good agreement with smog-chamber data, but there is still a tendency to over-predict the ozone concentration by around 50%.

Over the past few years the MCM was constantly upgraded to keep up with the growing body of mechanistic detail on aromatic oxidation provided by kinetic studies. The implemented mechanisms have been highly speculative in part, particularly for the ring-opening routes. Owing to a lack of data for model validation and of techniques to analyze the effects of new mechanistic details on the RO_x and NO_y budgets, on-line checks of the effects of these changes on the overall performance of the mechanism were not possible ($RO_x = OH + HO_2 +$ organic oxy radicals (RO) + organic peroxy radicals (RO_2); $NO_y = NO + NO_2 + NO_3 + HONO + HNO_3 +$ peroxy acyl nitrates (PAN_y) + organic peroxy nitrates (RO_2NO_2) + organic nitrates ($RONO_2$)). Thus, the procedure of mechanism development was hampered resulting in mechanisms that show large discrepancies in varying directions, if tested against recently available smog-chamber data.

This paper aims to give an overview of the status of toluene modelling based on a master chemical mechanism. Information on the major shortcomings of the current mechanism is derived from a comparison of model simulations with smog-chamber data. These shortcomings are tracked down to radical transformation within the mechanism. With the aid of a radical budget calculation, we identify the key intermediates that dominate radical production in smog-chamber toluene experiments and that provide the crucial information needed to develop future validation strategies. Furthermore, processes governing ozone production in the system are analysed and a sensitivity analysis is employed to identify the intermediates that have the highest impact on ozone production. The assembled information gives a precise description of areas where further research is needed to overcome current shortcomings in the mechanism and shows how modelling can become an interactive tool in mechanism development.

2   The mechanism

The toluene mechanism used for all calculations is extracted from the MCM v3 and has been modified according to recently available information on mechanistic details. In the following we will refer to this mechanism as TOL_MCM3a. A complete listing of reactions, rate coefficients and photolysis rates is available on the world wide web at http://www.chem.leeds.ac.uk/Atmospheric/intro.html. As for all VOCs treated by the MCM v3, the toluene mechanism is constructed according to a master chemical mechanism protocol (Jenkin et al., 2002). The framework of the mechanism is based on literature data on product yields, rate coefficients and photolysis rates of intermediates in the toluene oxidation system. Where no experimental data is available, kinetic

parameters are calculated using the principle of structure activity relationship (e.g. Atkinson, 1987; Kwok and Atkinson, 1995). Particularly for the ring-opening routes, the quantitative information on reaction products and their photochemical fate is still very scarce (Smith et al., 1998; Yu and Jeffries, 1997; Yu et al., 1997). Hence the implemented oxidation chemistry of these routes is very speculative.

Owing to the constantly growing amount of information on reactions relevant to toluene oxidation, it lies in the nature of any detailed mechanism that it remains always in an evolutionary state of development. For this reason the applied TOL_MCM3a mechanism shows deviations in a number of mechanistic details from the MCM v3. The only major differences that significantly affect radical production of the system are (1) photolysis of conjugated γ-dicarbonyls and (2) the oxidation of cresol.

1. In the MCM v3, generic photolysis rates are applied for the photolysis of conjugated γ-dicarbonyls derived from experimental data published by Sørensen et al. (1998), Liu et al. (1999) and Bierbach et al. (1994). For two γ-dicarbonyls, butenedial and 4-oxo-2-pentenal, which are oxidation products of toluene, experimental data are available (Sørensen et al., 1998) and we have set the photolysis rates for all γ-dicarbonyls in TOL_MCM3a accordingly. These changes result in a higher rate of production of RO_x radicals and generally increase the oxidation capacity of the toluene reaction system.

2. The OH-initiated oxidation of cresol in the MCM v3 is mainly described by a ring-opening route with a yield of 95%. Recent experiments on the reaction of OH with cresol have shown that the branching ratio for this route is far lower and depends strongly on the cresol isomer (Olariu et al., 2002). Based on this information we estimated an upper limit for the ring-opening route for the reaction of OH with cresol of 28% and changed the mechanism in the TOL_MCM3a model accordingly. The products of the ring-retaining routes are multifunctional compounds containing a combination of -NO_2, -ONO_2 and -OH groups. The main effect of the higher branching ratio for ring-retaining products is therefore a sequestering of NO_x into nitro- and nitroxy-aromatics, which in turn means a lower O_3 production potential of the aromatic oxidation system. Furthermore, reactions of NO_3 with cresol and its substituted isomers are implemented. These reactions become an important sink for cresol and for NO_x in the later stages of smog-chamber experiments when, due to low NO levels, the NO_3 concentration increases to some pmol/mol.

In TOL_MCM3a, toluene oxidation is represented by 229 species and 676 reactions, describing the breakdown of the carbon skeleton. The OH-initiated oxidation of toluene proceeds via 5 reaction channels, which are labelled according

to the most prominent reaction products (Fig. 2). The dicarbonyl and the epoxide routes proceed via opening of the aromatic ring in the first reaction step. The branching ratio has not been measured for either of these routes. In the model they together account for 67% of the total toluene oxidation that is not covered by ring-retaining routes. Based on available data a dicarbonyl:epoxide ratio of 7:3 was adopted, reflecting the different amounts of experimental evidence for the two routes.

In the dicarbonyl route the aromatic ring breaks down into α-dicarbonyls (glyoxal and methylglyoxal) and co-products that are represented by conjugated γ-dicarbonyls (butenedial, 2-methylbutenedial and 4-oxo-2-pentenal) and furanones (2(5H)-furanone and β-angelicalactone). The epoxide route results in the formation of 2,3-epoxy-6-oxo-4-heptenal (in the following labelled epoxide-1) as the primary product. The first generation products of the ring-opening routes are gradually further oxidized resulting in higher oxygenated compounds with a declining number of carbon atoms, eventually producing HCHO, CO and CO_2. Owing to the limited experimental information available for these routes the implemented chemistry is a major area of uncertainty in the current mechanism.

The ring-opening pathways of the toluene oxidation proceed by a sequential addition of OH and O_2 resulting in a hydroxycyclohexadienyl type peroxy radical (Fig. 1). Depending on the NO concentration there are three proposed reaction pathways for this radical: (1) a cyclisation to form a peroxide bridged radical which is the precursor for both the carbonyl and the epoxide route (Jenkin et al., 2002), (2) an isomerisation and subsequent release of HO_2 to form cresol and (3) the reaction with NO resulting in the production of an oxy-radical that undergoes ring-opening and eventually results in the formation of muconaldehyde-type compounds. Ghigo and Tonachini (1999) and Motta et al. (2002) have investigated the photooxidation of benzene in theoretical studies. They both came to the conclusion that the NO promoted pathway can only compete with the cyclisation under polluted conditions. For NO concentrations of about 100 nmol/mol Ghigo and Tonachini (1999) estimate a branching ratio for the NO pathway of less than ten percent. Although this value was calculated for benzene, it can be taken as a tentative indication that the muconaldehyde route for aromatics in general is only of importance at NO_x concentrations in the μmol/mol range. This is in line with experimental studies at moderate NO_x levels in which only qualitative evidence for muconaldehyde type compounds as minor reaction products in the toluene system was found (Yu et al., 1997). On the basis of the results of the theoretical studies and the weak experimental evidence for the muconaldehyde route in the toluene system this reaction pathway is not implemented in the MCM v3.

The three ring-retaining routes are labelled cresol, benzaldehyde and quinone. The cresol route has a significant effect on the NO_x budget as it sequesters NO_2 and NO_3 into nitro-aromatics. Only 28% of cresol is further degraded by a ring-opening route to glyoxal and 4-oxopentenoic acid. The benzaldehyde and quinone routes are of only minor importance for toluene oxidation, due to their comparatively low yields. Benzaldehyde is the only first generation product that has no significant ring-opening channel, but, about 6% is further converted to nitrophenol by elimination of CO. In the quinone route the oxidation of methyl-1,4-benzoquinone results in a variety of multioxygenates, which break down further to yield predominantly CO and HCHO.

3 Model experiment comparison

3.1 The smog-chamber experiment

Owing to the complexity of the photooxidation of aromatics, only one-component experiments are suitable for the validation of aromatic mechanisms. The number of toluene-NO_x experiments available is still very scarce. The experiment providing the most suitable dataset is the 22/10/97 toluene-NO_x system studied at the large-volume outdoor smog-chamber EUPHORE, located in Valencia, Spain. The hemispherical chamber consists of FEP (fluorine ethene propene) foil and has a volume of 195.5 m^3. The experiment was conducted as a classical smog-chamber run in which toluene (482 nmol/mol) and NO (134 nmol/mol) were injected into the dark chamber. To start the reaction the protective housing was retracted so that the chamber was exposed to sunlight photoinitiating the toluene oxidation. The concentrations of toluene, NO, NO_2, and ozone were measured with a FTIR Spectrometer (Nicolet Magna 550) in combination with an open path white cell (optical path length, 526 m). For the measurement of the photolysis rates of O_3 NO_2, HCHO and HONO a spectroradiometer (Bentham DM300) was employed.

3.2 The model simulation

For the simulation of the 22/10/97 experiment the model was initialised with concentrations of toluene, NO, NO_2 and HONO. The high NO concentrations in the chamber at the point of NO injection led to production of NO_2 by a termolecular reaction ($2 NO + O_2 \rightarrow 2 NO_2$), giving an initial concentration of NO_2 in the chamber of 14 nmol/mol. Another side effect of the injection of NO into the chamber is the production of traces of HONO, which is almost certainly generated from the reaction of the newly formed NO_2 at the chamber wall (see discussion in Sect. 4.2). In the 22/10/97 experiment the initial HONO concentration was below the detection limit of the FTIR instrument of around 5 nmol/mol. From earlier experiments in which HONO formation has been investigated, we know that the initial HONO concentration depends on the history of the chamber and the NO_x loading. Based on information from those chamber characterisation studies we have estimated a HONO background
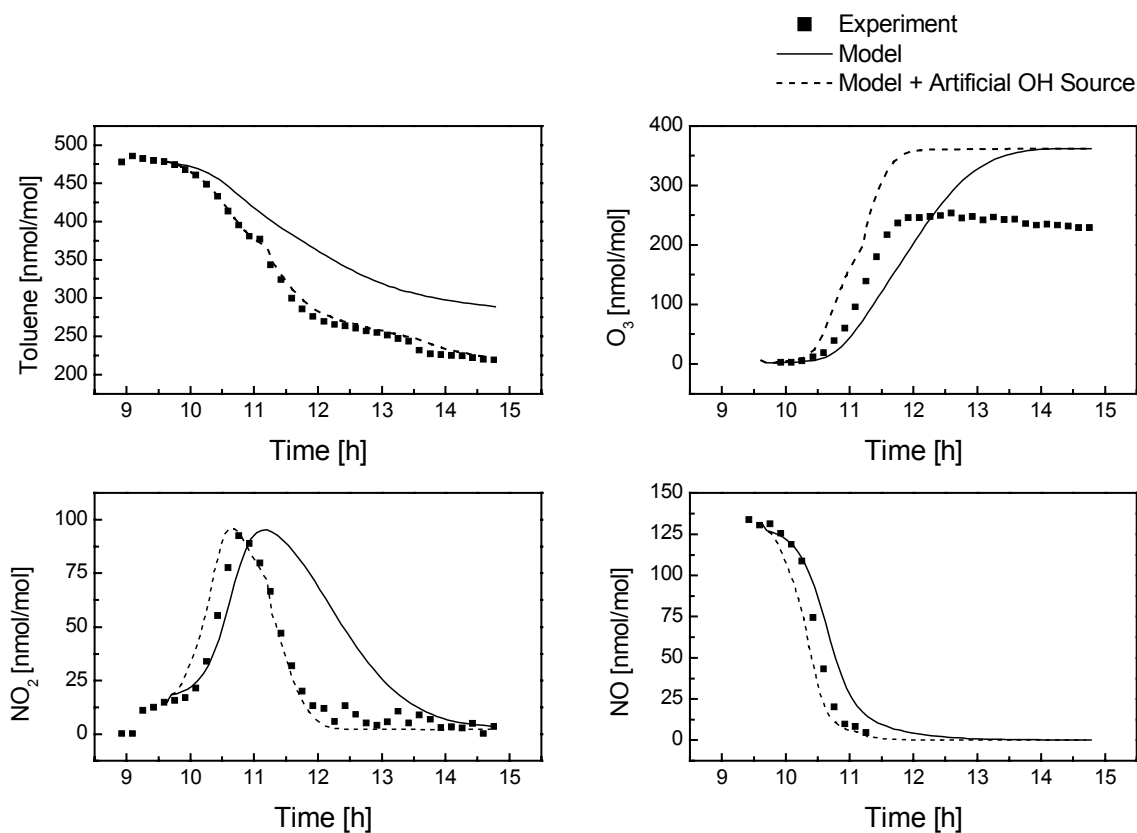
Fig. 3. Experimental and simulated concentration-time profiles for the toluene-NO$_X$ experiment 22/10/97 carried out at the EUPHORE chamber. Also shown, a model run in which an artificial OH source has been implemented in the model. The OH source strength has been tuned so that the modelled toluene decay matches the experimental values (see text).

concentration of 0.5 nmol/mol for the 22/10/97 experiment and have initialised the model accordingly.

For O$_3$, NO$_2$, HCHO and HONO measured photolysis rates were taken for the model simulation. For all other photolysis processes, the corresponding boundary layer photolysis rates were calculated for the chamber location and experiment date, as described elsewhere (Saunders et al., 2002; Jenkin et al., 2002). These calculations do not consider the actual cloud coverage, the backscattering of the chamber floor and the transmission of the chamber FEP film. Therefore we have adjusted the calculated photolysis rates with a factor that is based on the average deviation between measured and calculated photolysis rates for O$_3$, NO$_2$, HCHO and HONO.

The results of the model-experiment comparison are shown in Fig. 3. The model predicts a toluene decay that is about 28% too low compared to the experiment, corresponding to a severe model under-prediction of the OH concentration (for all model experiment comparisons the experimental value is taken as 100%). Despite the lower oxidation capacity, the model over-predicts the ozone concentration at the end of the experiment by about 55%. NO$_2$ concentrations are substantially higher than measured for the period after

NO$_2$ has reached its maximum, in agreement with the model ozone over-prediction. The comparatively good agreement in the first 1.5 h indicates that in the early stages of the experiment, when the chemistry of the system is dominated by the initial oxidation step of toluene, the NO to NO$_2$ conversion is well represented in the model. This conclusion is also supported by the good agreement between the experimental and simulated NO concentration-time-profile within the first hour. In the later stages of the experiment the oxidation of first and higher generation products becomes increasingly important. Shortcomings in the implemented chemistry of these compounds are probably responsible for the observed discrepancies in the O$_3$ and NO$_2$ concentration-time profiles.

3.3 Product yields

Mechanistic and observed product yields for first generation products in the toluene system are compiled in Table 1. The cresol yields reported in 12 studies vary between 12% and 38.5% (Klotz et al., 1998, and references therein). In the model only one surrogate compound is implemented that represents all three isomers of cresol. The mechanistic yield of 20% for this compound comes close to experimental values

Table 1. First generation product yields in the toluene system: comparison between model and literature data

Intermediate	Yield (%)		Reference
	Model	Literature	
o-Cresol	20.0	12–38.5	[7]
m- + p-Cresol	–	4.8–5.9	[4, 7]
Benzaldehyde	6.0	5.4–12	[4, 7]
Glyoxal	23.8	8–39	[4, 5]
Methylglyoxal	23.8	7.5–16.7	[2, 4]
Butenedial	11.9	Detected	[1, 2]
4-Oxo-2-pentenal	7.9	3.1	[2]
2-Methylbutenedial	7.9	Detected	[8]
2(5H)-Furanone	11.9	Proposed	[3]
α-Angelicalactone[a]	7.9	2.9	[2]
2,3-Epoxy-6-oxo-heptenal	20.0	Evidence	[6]
Methyl-1,4-benzoquinone	4.6	Detected	[1]

[a] In the model represented as β-angelicalactone.
References are as follows: [1] Yu et al., 1997; [2] Smith et al., 1998; [3] this work; [4] Atkinson, 1992; [5] Volkamer et al., 2001, and references therein; [6] Yu and Jeffries, 1997; [7] Klotz et al., 1998, and references therein; [8] Jang and Kamens, 2001.

published more recently by Klotz et al. (1998) and Smith et al. (1998). For benzaldehyde, the spread in literature yields is a factor of two and the model gives a yield of 6% that is supported by several studies published in the nineties by Klotz et al. (1998), Bierbach et al. (1994), and Seuwen and Warneck (1996). Literature values for the glyoxal yield vary between 8% and 39% (Atkinson, 1992; Volkamer et al., 2001 and references therein). This spread of more than a factor of four indicates high experimental uncertainties. In the model only the dicarbonyl route, with a branching ratio of 48%, yields glyoxal and methylglyoxal as first generation products. According to the different possible symmetries of the peroxide-bicyclic intermediate, and the different positions where the ring of this radical can break, there are 5 ring-opening routes implemented in the model. They result either in the formation of glyoxal and a C_5 co-product or methylglyoxal and a C_4 co-product. The branching ratios for the C_4 and C_5 pathways is set to 50% giving yields of 23.8% for both, glyoxal and methylglyoxal. The yields most recently published are higher for glyoxal but lower for methylglyoxal with 39% and 16.7% respectively (Volkamer et al., 2001; Smith et al., 1998). This indicates that the glyoxal route is the favoured ring-opening pathway and the combined branching ratio of the two routes might be some percent higher than currently implemented in the model. However, the uncertainties in the measured yields are still very high, and they should be confirmed by further studies before the mechanism is adjusted

accordingly.

The co-products of glyoxal and methylglyoxal are represented in the model by three γ-dicarbonyls, butenedial, 2-methylbutenedial, 4-oxo-2-pentenal, and two furanones, 2(5H)-furanone and α-angelicalactone. They result from applying a set of rules, based on structure activity relations, to the breakdown of possible isomers of the peroxide-bicyclic intermediate. Only two of the co-products, α-angelicalactone and 4-oxo-2-pentenal, could be quantified in laboratory experiments (Smith et al., 1998), while qualitative evidence exists for two further co-products, butenedial and 2-methylbutenedial (Yu et al., 1997; Smith et al., 1998; Jang and Kamens, 2001). 2(5H)-furanone has only been proposed and not observed (this work). If we assume a glyoxal yield of 39%, as suggested by measurements of Volkamer et al. (2001), only 15% of the possible co-products could be quantified in laboratory experiments (Smith et al., 1998). The poor carbon balance shows that the degradation chemistry of the dicarbonyl route is still a major area of uncertainty in the understanding of toluene oxidation chemistry. The most speculative reaction channel is the epoxide pathway, currently implemented with a yield of 20%. For this reaction channel and putative oxidation products only qualitative evidence could be found so far (Yu and Jeffries, 1997).

4 The radical budget

4.1 Procedure

The hydroxyl radical, as dominant oxidant, defines the oxidation capacity in the toluene system. Thus, the net effect of an intermediate on the OH radical budget is a reliable measure for its contribution to the oxidation capacity of the system. However, OH is in a quasi steady state so that, while its production and sink terms are of the order of 10^{-2} nmol/mol s^{-1}, the net OH production is only around 10^{-7} nmol/mol s^{-1}. A calculation of the net production by taking the difference between sink and production terms at short time scales is thus beyond the precision of the numerical integration process. However, the production of new radicals is the key process feeding the radical chain and maintaining high radical levels in the system, in competition with the radical sink processes, such as reaction of OH with NO_2 and peroxy-peroxy radical termination. For this reason, new radicals produced by a compound or a reaction channel provide a good measure of its effect on the overall oxidation capacity of a reaction system.

The photooxidation of a generic VOC involves the following radical transformation sequence (e.g. Jenkin and Clemitshaw, 2000): the oxidation is initiated by reaction of OH with the VOC; the net effect is a conversion of OH into RO_2 (see also Fig. 4). RO_2 propagates by reaction with NO to RO, which in turn reacts with oxygen to produce HO_2 and a carbonyl compound. The cycle is closed by the conversion of
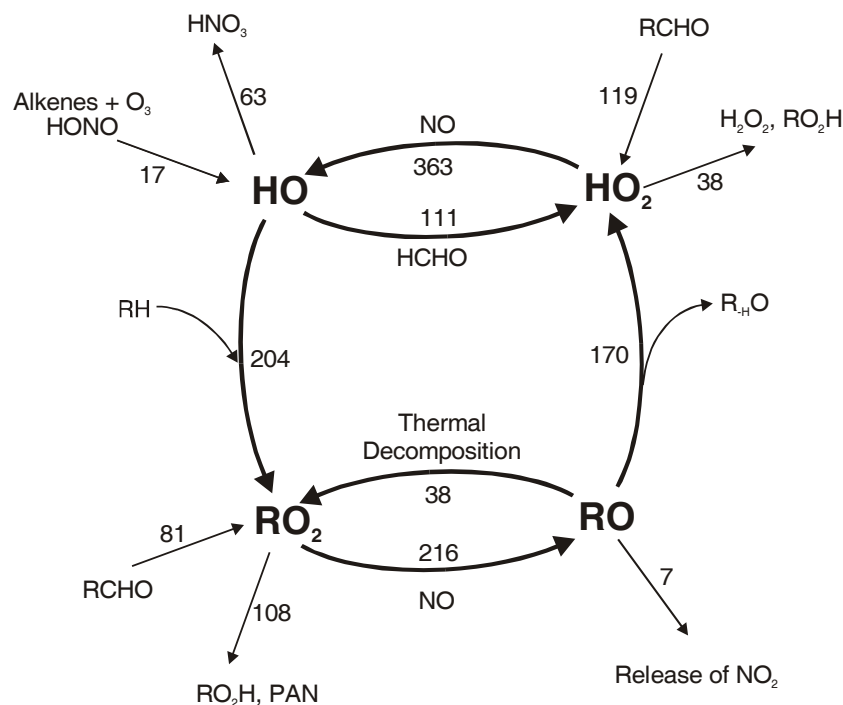
Fig. 4. Schematic representation of the RO_x cycle in the toluene system, showing major routes of transformation between OH, RO_2, RO and HO_2 radicals and source and sink processes for each RO_x species. The numbers are total flows through the transformation channels in units of nmol/mol calculated for the entire time of the toluene-NO_x experiment 22/10/97.

HO_2 back into OH by reaction with NO. Major sources of RO_x radicals are the photolysis of aldehydes and the reaction of O_3 with alkenes. Radicals are removed from the reaction system by termination processes such as reaction of OH with NO_2 and peroxy-peroxy radical termination. Based on this fundamental description of the radical transformation in photochemical systems we have calculated the RO_x budget for the 22/10/97 toluene experiment. We applied the following definitions and procedures, which enabled us to consider all radical conversion processes in the toluene mechanism:

1. New radical production is defined as breakdown of a closed shell molecule into two radical species or a transformation of NO_3 into a RO_x species. As stated above, the most abundant processes of new radical production are photolysis of carbonyls and ozonolysis of alkenes. Furthermore the reaction of NO_3 with VOC produces RO_x radicals and thus acts as a link between the NO_x and RO_x radical families. RO_2 production through reactions such as $RH + NO_3 + O_2 \rightarrow RO_2 + HNO_3$ is also classified as new radical production.

2. Propagation is the transformation of one RO_x species into another RO_x species.

3. Termination is defined as combination of two radicals to form a closed shell molecule.

4. For compounds that are in a fast equilibrium with radicals, net terms are calculated. For example, the thermal decomposition of PAN-type compounds is not taken as

radical production, but subtracted from the $RC(O)O_2 + NO_2$ consumption term.

5. Compounds that are produced by radical radical combination and that then break down into radicals of another type (e.g. hydroperoxides) are defined as temporary reservoirs and their breakdown is taken into account as "delayed" radical propagation. These processes account for less than 1% of the major radical propagation routes under conditions of the 22/10/97 experiment. Therefore they are not treated separately, but added to the major radical conversion routes, according to the net effect the delayed radical propagation has on the RO_x budget.

RO_2 and HO_2 account for a large fraction of the newly produced radicals in the reaction system, but only the portion of them that is converted into OH contributes to the oxidation capacity of the system. For this reason we define OH equivalents as the fraction of HO_2 or RO_2 that is effectively transformed into OH:

$$[OHeq]_{HO_2} = \gamma_{HO_2} \cdot [HO_2], \tag{1}$$

$$[OHeq]_{RO_2} = \gamma_{RO_2} \cdot [RO_2], \tag{2}$$

where γ_{HO_2} and γ_{RO_2} represent the conversion factors from one radical species into OH:

$$\gamma_{HO_2} = \frac{HO_2 \text{ conversion to OH}}{\text{total } HO_2 \text{ consumption}}, \tag{3}$$

$$\gamma_{RO_2} = \gamma_{HO_2} \frac{RO_2 \text{ conversion to } HO_2}{\text{total } RO_2 \text{ consumption}}. \tag{4}$$
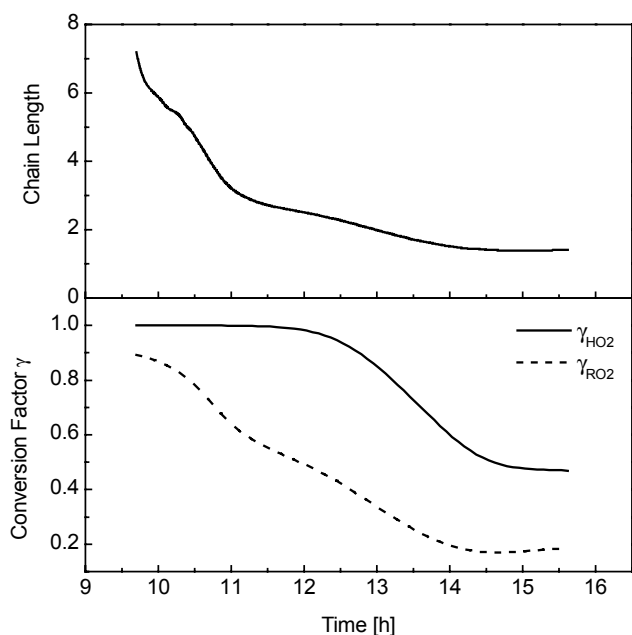
Fig. 5. Time profiles for chain length and conversion factors γ calculated for the toluene-NO_x experiment 22/10/97. The conversion factor γ is defined as the fraction of a radical species (RO_2 or HO_2) that is converted into OH.

Fig. 6. Total new OH (ΣOH_{new}) production and termination in reaction channels of the toluene system, calculated over the course of the 22/10/97 experiment. Initiation and termination of HO_2, RO_2 is considered in terms of OH equivalents (see text).

Total new OH (ΣOH_{new}) is then defined as the sum of new OH and OH equivalents from new HO_2 ([new $OHeq]_{HO_2}$) and new RO_2 ([new $OHeq]_{RO_2}$):

$$\Sigma OH_{new} = [\text{new OH}] + [\text{new OHeq}]_{HO_2} \\ + [\text{new OHeq}]_{RO_2} . \quad (5)$$

With this definition we can finally calculate the effective chain length of the radical cycle in the toluene system, which is the average number of times a newly created OH radical will be recreated through radical chain propagation before it is destroyed:

$$n(OH) = \frac{\Sigma OH_{new} + \text{propagated OH}}{\Sigma OH_{new}} . \quad (6)$$

The OH chain length is an important parameter for smog-chamber experiments that gives information about the relative importance of radical production to the total radical turnover in the system.

Classification of all reactions and subsequent calculation of the RO_x budget for the toluene system is a prerequisite to compute the conversion factors for HO_2 and RO_2 into OH and hence, the contribution of a compound or reaction channel to ΣOH_{new}. These calculations enable us to identify the compounds and reaction channels that dominate the oxidation capacity of the system and which are most likely to be responsible for the current shortcomings in the toluene mechanism.
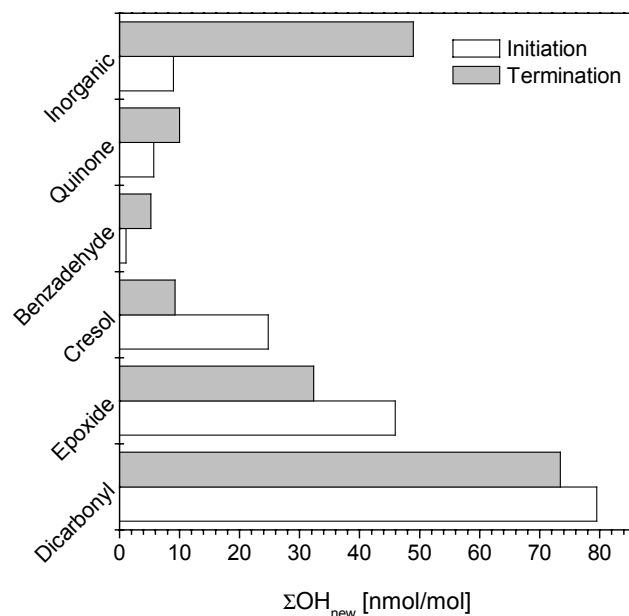
4.2 The OH budget

The calculated radical fluxes in the toluene-NO_x system 22/10/97 are shown in Fig. 4. They are given as amount of radicals, in units of nmol/mol, that follow each pathway over the entire time of the simulation. New OH production is about 17 nmol/mol from ozonolysis of alkenes and photolysis of HONO that is formed by reaction of NO_2 on the chamber walls. 119 nmol/mol of new HO_2 is produced, mainly by the photolysis of aldehydes, and 81 nmol/mol RO_2 is created, with photolysis of aldehydes and ozonolysis of alkenes as major sources. 63 nmol/mol of OH is directly lost via reaction with NO_2 and PAN-type compounds and a further 153 nmol/mol of RO_x is lost by various sink reactions, such as formation of hydroperoxides, peroxy-peroxy permutation reactions and formation of nitrates. Applying the transformation factors, we calculate a ΣOH_{new} production of 162 nmol/mol over the course of the experiment, with a contribution of new OH equivalents from HO_2 and RO_2 of 107 nmol/mol and 38 nmol/mol, respectively. The calculations were carried out as a function of time to investigate the time dependencies of the chain length and conversion factors. At the beginning of the experiment the chain length is 7.2 and the conversion factors γHO_2 and γRO_2 are 1 and 0.9, respectively (Fig. 5). The high NO concentration allows radical propagation to dominate sink processes and the radicals cycle several times between the different radical types before they are destroyed by termination reactions. As [NO] decreases and [RO_x] increases, HO_2 and RO_2 combination

Table 2. Total new OH (ΣOH_{new}) and NO to NO_2 conversion in reaction channels of the toluene system, calculated for the toluene-NO_x experiment 22/10/97

| Reaction channel | Branching ratio | Per molecule toluene oxidized | | | Per molecule NO_2 consumed |
		Total new OH	NO to NO_2 conversion	NO_x consumed	NO to NO_2 conversion
Dicarbonyl	0.48	1.1	4.7	0.69	6.8
Epoxide	0.2	1.5	4.9	0.90	5.5
Cresol	0.2	0.7	2.4	0.88	2.8
Benzaldehyde	0.07	0.1	1.3	0.41	3.1
Quinone	0.05	0.7	3.7	0.65	5.8

processes become more important and the chain length continuously decreases over the course of the experiment. By the end of the experiment, [NO] has dropped to 0.1 nmol/mol resulting in a chain length of 1.4 and conversion factors for HO_2 and RO_2 of 0.48 and 0.17, respectively.

To assess the importance of the major reaction channels to the oxidation capacity we calculated ΣOH_{new} production and consumption separately for each of them. The results show that the dicarbonyl, epoxide and cresol routes act as radical donors in the system as their radical production terms are higher than their sink terms (Fig. 6). The benzaldehyde, the quinone route and the inorganic chemistry (mainly the reaction of NO_2 + OH) have sink terms that are higher than their production terms. The largest contribution to the total new OH production comes from the dicarbonyl route with 80 nmol/mol ΣOH_{new}. Table 2 shows the number of ΣOH_{new} radicals produced per toluene molecule oxidized for each channel. The dicarbonyl and the epoxide routes are most efficient in producing ΣOH_{new} as they break down into a number of carbonyl compounds, which photolyse and produce radicals in high yields. The quinone and cresol routes have a lower efficiency in producing radicals as in the first generation products the aromatic ring is retained. Thus, ring-opening occurs a reaction sequence later and the ring-opening products are more oxidized and show less propensity to produce radicals. The benzaldehyde route has no significant ring-opening channel and the net radical production of the photolysis of benzaldehyde is relatively low as the corresponding acyl peroxy radical sequesters NO_x efficiently by forming peroxybenzoyl nitrate. Through removing NO_x the chain length is decreased, which compensates to a large extent the new radical production by the initial photolysis of benzaldehyde. Apparently, ring-opening is a prerequisite for a strong radical production in a reaction pathway, as ring-retaining oxidation processes do not provide enough aldehydes, which act as efficient radical sources.

Table 3 shows the 11 most important radical sources in the toluene system that produce about 80% of ΣOH_{new}. Apart from HCHO, all compounds are solely or predominantly

formed in first generation processes. Owing to a combination of a high yield and high photolysis rates, methylglyoxal is the strongest radical source followed by epoxide-1 and glyoxal. Furthermore, the conjugated γ-dicarbonyls (4-oxo-2-pentenal, butenedial, and 2-methylbutenedial) and furanones (2(5H)-furanone and α-angelicalactone), which represent the co-products of glyoxal and methylglyoxal, are also of major importance, contributing 25% to ΣOH_{new}. The photolysis of HONO, which is produced by wall reactions of NO_2, accounts for 9 nmol/mol of the newly produced OH over the course of the experiment.

The analysis of the radical budget also gives information on the importance of chamber effects for the radical turnover in a toluene experiment. Based on characterisation measurements at the EUPHORE chamber the radical production caused by wall reactions can be described by a process in which gas-phase NO_2 is transformed into HONO. Thus, the rate of HONO production on the walls is a function of the NO_2 concentration in the chamber. For this process ($NO_2 \rightarrow$ HONO) an average rate coefficient $k_{HONO,wall}$ of $(1.15\pm0.45)\times10^{-5}\,s^{-1}$ has been established for the EUPHORE chamber. Unfortunately HONO formation is not a constant but also depends on the history of the chamber, so that the actual source strength of HONO production for a particular experiment is not known. However, the average value for $k_{HONO,wall}$ gives a good first guess for wall production of HONO and was used in the simulations of the 22/10/97 experiment.

Over the whole course of the 22/10/97 experiment the total OH production by the photolysis of HONO resulting from wall reactions is only 9 nmol/mol compared to a ΣOH_{new} production in the toluene system of 153 nmol/mol. Even if we double the rate constant for the conversion of NO_2 to HONO, OH production by chamber effects would be only of the order of 12% of the ΣOH_{new} production of the toluene system.

For conditions such as those in the 22/10/97 experiment the effect of wall produced radicals on the OH production in the early and middle stages of the experiment is certainly

Table 3. Total new OH (ΣOH_{new}) production by compounds over the course of an experiment. Calculated for the toluene-NO_x experiment 22/10/97

Compound	ΣOH_{new} (nmol/mol)	Contribution to ΣOH_{new} in toluene system (%)
Methylglyoxal	24.4	15.1
Epoxide-1	24.1	14.9
Glyoxal	14.9	9.2
4-Oxo-2-pentenal	12.6	7.8
Butenedial	10.4	6.4
Cresol	8.7	5.4
HONO	8.4	5.2
HCHO	7.6	4.7
α-Angelicalactone	7.6	4.7
2-Methylbutenedial	5.2	3.2
2(5H)-Benzofuranone	5.1	3.2
Sum		79.8

minor and cannot explain the model-experiment discrepancies in the OH production and the toluene decay. However, as over the course of an experiment a complex mixture of highly reactive organics and NO_y species are transferred to the walls, at the end of an experiment (final 1.5 h) the situation becomes more uncertain. There might be a variety of wall related processes producing radicals, which so far have not been considered. Therefore, it cannot be ruled out that at the end of an experiment chamber effects have indeed a significant impact on the radical production in the system.

4.3 Time profiles of new OH production

To quantify the missing OH production in the model we implemented an artificial OH source and tuned the source rate so that exactly the amount of OH is injected into the system that is needed to match the measured toluene decay. From this procedure we showed that an additional 300 nmol/mol OH is necessary over the course of an experiment to bring the simulated and experimental toluene decays into agreement. This means that the modelled OH production of 380 nmol/mol (see also Fig. 4) is around 44% too low compared to the experiment.

A more detailed picture of the nature of the missing OH source can be derived from the time dependencies of OH sources in the system. If we consider the discrepancies from a model point of view it becomes clearer how much the OH production in the model has to be increase to match the radical production in the experiment. The time profiles in Fig. 7 show that, at all times during the experiment, ΣOH_{new} production in the model is too low by at least 25% (model OH
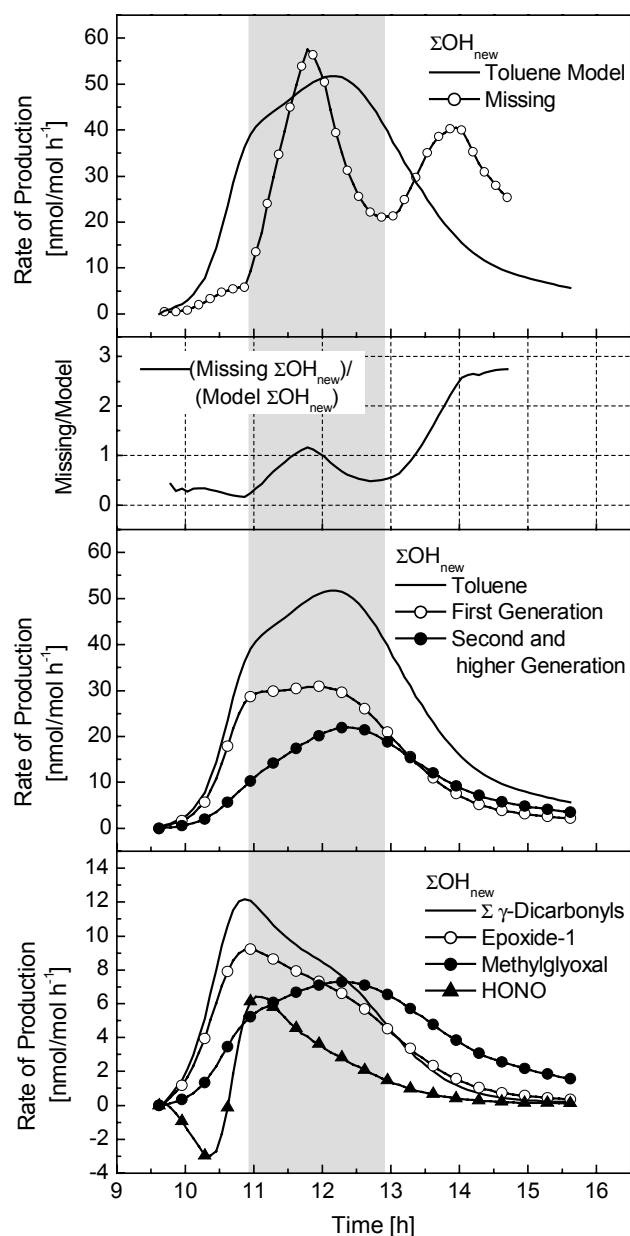

Fig. 7. Time profiles for OH production: (1) Modelled total new OH (ΣOH_{new}) production in the toluene system and missing ΣOH_{new}. (2) Missing ΣOH_{new} as fraction of modelled ΣOH_{new}. (3) Contributions of first and second generation products to ΣOH_{new}. (4) ΣOH_{new} produced by strongest radical sources in the reaction system. Grey area indicates the time period when the missing OH shows a distinct maximum suggesting a strong radical source that is not yet implemented in the model.

is taken as 100%). Around 12:00 the ΣOH_{new} production in the experiment is about a factor of two higher than in the model and in the final 1.5 hours of the experiment the deviation increases to about a factor of three. Panel 3 of Fig. 7 shows that, in the model, first generation products dominate ΣOH_{new} production until about 12:00. In the latter stages of

the experiment second generation products gain more importance, making up about 60% of ΣOH_{new}.

The time profiles of ΣOH_{new} production differ significantly depending on the photo-chemical reactivity of a compound (Fig. 7, panel 4). The photolysis of small amounts of "background" HONO (an estimated 0.5 nmol/mol), produced during the injection of NO into the chamber, initiates the photochemistry in the toluene-NO_x system. Once initial HONO is photolysed the recombination reaction of NO with OH to HONO becomes a net sink for OH. After one hour of reaction time, when significant amounts of NO have been converted into NO_2 so that HONO formation on the walls increases and OH loss via reaction with NO becomes less important, HONO is again a net source of radicals. An important result of the OH production analysis is that conjugated γ-dicarbonyls and epoxide-1 are essential for OH production in the early stages of the experiment. Methylglyoxal and glyoxal, both first generation products, are strong radical sources in the system but the radical production rate is initially too slow to explain the high OH concentration at the beginning of the experiment.

From the analysis of the time profiles of ΣOH_{new} production we can conclude that a general increase of the "background" production rate for ΣOH_{new} of about 25% in the model is necessary to describe the oxidation capacity in the experiment. At 12:00, when [OH] in the system peaks, a distinctive increase of the radical production in the model is necessary. An increase in the photolysis rates of conjugated γ-dicarbonyls or epoxide-1 to reproduce this OH peak would necessarily lead to an overestimation of the reactivity at the beginning of the experiment, whereas an increase in the ΣOH_{new} production rate of second and higher generation products would produce an OH peak that is too late. The analysis of the time profiles suggests a strong radical source that is not yet implemented in the mechanism and that produces new radicals in a period between the peaks of the ΣOH_{new} production rates corresponding to the photochemistry of first and second/higher generation products. As pointed out above, the nature and the photochemical fate of the co-products of glyoxal and methylglyoxal and the intermediates in the epoxide route are a major area of uncertainty in the toluene mechanism. Hence, it is very likely that these parts of the mechanism are responsible for the observed discrepancies between modelled and experimental OH production in the early and middle stages of the experiment.

In the last two hours of the experiment the modelled OH production is too low by 55 nmol/mol. Because of low [NO] at the end of the experiment, the conversion factors for HO_2 and RO_2 are less than 0.5 and the rate of production of new radicals in the system has to be more than tripled to explain the measured toluene decay. This points to a severe lack of understanding of the chemistry in the latter stages of the experiment, when reaction products of the toluene oxidation become increasingly important as reaction partners for OH. The situation becomes even more intricate as the effect of
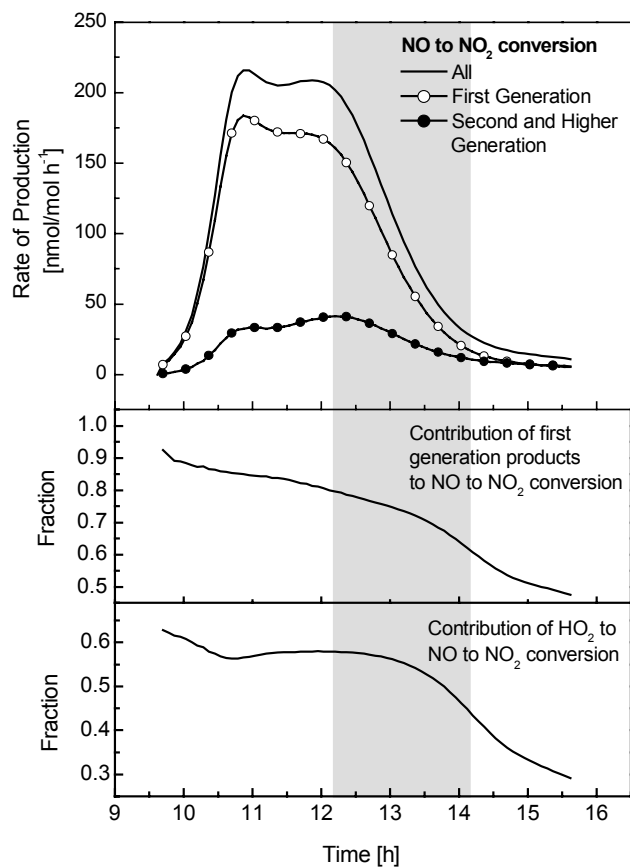

Fig. 8. Rate of NO to NO_2 conversion calculated for toluene-NO_x experiment 22/10/97. Panel 1: Time profile of NO to NO_2 conversion, all processes, reactions of first generation products and reactions of higher generation products. Panel 2: Contribution of first generation products to NO to NO_2 conversion. Panel 3: Contribution of HO_2 to NO to NO_2 conversion. Grey area indicates time period where the model over-predicts the O_3 production in the experiment.

wall related reactions on the radical budget in the chamber is more uncertain at the end of the experiment owing to the complex mixture of organics and the high concentration of NO_2 and HNO_3 transferred to the walls over the course of the experiment. Further research is necessary to find out whether highly oxygenated reaction products or chamber wall related effects are responsible for the high radical production in the latter stages of the experiment.

5 Ozone chemistry

5.1 Excess ozone

The model over-prediction of the experimental ozone concentration in the 22/10/97 experiment is directly linked to the NO_x chemistry and is reflected by an over-prediction of measured [NO_2]. An increase in the OH concentration so

that the simulated toluene decay matches the experimental decay leads to faster chemistry and a more rapid build-up of ozone, but, $[O_3]$ at the end of the experiment is virtually unaffected (Fig. 3). As ozone is produced by the photolysis of NO_2, the influence of reaction channels or of intermediates on ozone production is determined indirectly by their efficiency in converting NO into NO_2. The second important parameter, which has a major effect on ozone production, is the conversion of NO_x into sinks, such as HNO_3 and PAN, which are stable over the time scale of the experiment. The capacity of a reaction channel to produce ozone is thus a function of its capacities to convert NO to NO_2 and to sequester NO_x into stable nitrogen compounds.

Table 2 shows that the dicarbonyl and epoxide routes are most efficient in converting NO to NO_2. They produce 4.7 and 4.9 molecules NO_2, respectively, per molecule of toluene oxidized. The benzaldehyde route with a branching ratio for ring-opening of less than 1% produces only few peroxy radicals and NO_2 production is consequently very low with 1.3 molecules per molecule toluene oxidized. The epoxide and cresol routes show the largest efficiency for NO_x consumption, removing 0.90 and 0.88 molecules NO_x, respectively, per molecule toluene oxidized. In the epoxide route the main sinks for NO_x are HNO_3 and PAN whereas in the cresol route the formation of nitro-hydroxy aromatics is most important. As a measure of the efficiency of ozone production we have calculated the number of NO to NO_2 conversions per molecule NO_x consumed. This number is highest for the dicarbonyl route as this route shows a strong NO to NO_2 conversion in conjunction with a limited capacity to sequester NO_x into stable NO_y species. Cresol shows the lowest value owing to a small branching ratio for ring-opening and a high conversion of NO_x into nitro-hydroxy aromatics.

The toluene mechanism contains 166 reactions converting NO to NO_2, with 41 reactions accounting for 80% of the NO_2 production. For simplification, we have lumped all processes into two groups relating respectively to the creation or oxidation of first generation products and to the oxidation of second or higher generation products. Figure 8 shows that, over the first 2.5 h of the experiment, more than 80% of the NO to NO_2 conversion is caused by the production or by the oxidation of first generation products. In the time window when the model starts to over-predict the O_3 production, from 12:30 until 14:30, the contribution of first generation products drops from 80 to 60% and the chemistry of secondary products becomes more important. Furthermore the NO to NO_2 conversion by RO_2 gains in importance. While at the beginning of the experiment more than 60% of the NO_2 is produced by reaction of NO with HO_2, its contribution drops to around 40% at 14:30. From this analysis we can conclude that during the time period when the model over-predicts ozone production, the chemistry that is linked to first generation products accounts, on average, for about two thirds of the total NO to NO_2 conversion.

One option to correct the excess ozone formation would

Table 4. NO_y budget calculated for the toluene-NO_x experiment 22/10/97. Concentrations of NO_y species are given for the end of the experiment at 15:00. Compounds are arranged into a group of "accessible" NO_y species that can be measured with standard analytical equipment and a group of "problematic" NO_y species, for which quantification is a major analytical challenge

NO_y Compound	Concen-tration (nmol/mol)	Contribution to total NO_y (%)	Comment
Accessible			
HNO_3	41.7	31.1	
PAN	34.2	25.5	
NO_2	3.9	2.9	
Nitrocresol	0.5	0.4	
Total		59.9	
Problematic			
Nitro-aromatics	22.1	16.5	7 compounds
PAN_y	18.4	13.7	14 compounds NO_2 to HNO_3
Wall	8.7	6.5	conversion on walls
Other	4.6	3.5	NO_y in aerosols

be to reduce the production of peroxy radicals, but this would also reduce OH formation and thus conflicts with the need to increase the oxidation capacity in the system. Therefore we suggest two processes that are likely to be responsible for the over-prediction of O_3 by the model:

1. A missing source of OH involving no, or with only little, NO to NO_2 conversion, such as ozonolysis of alkenes or isomerisation of peroxy-radicals in a similar mechanism to that during dimethyl ether oxidation as suggested by Jenkin et al. (1993). For example, for the latter, the peroxide-bicyclic peroxy radical, proposed as intermediate in the dicarbonyl route, could isomerise and break down, directly generating OH and α- and γ-dicarbonyls. This ring-opening mechanism does not include the two NO to NO_2 conversions of the classical reaction sequence in which a peroxy radical is transformed into a carbonyl compound and OH.

2. NO_3 chemistry as a possible means of sequestering reactive nitrogen species by forming stable NO_y compounds and at the same time producing RO_x radicals (Wayne et al., 1991). The addition of NO_3 to a double bond or an aromatic ring and subsequent reaction of the adduct with O_2 can lead to a reaction sequence in which NO_3 is tied-up into a nitrooxy-compound and
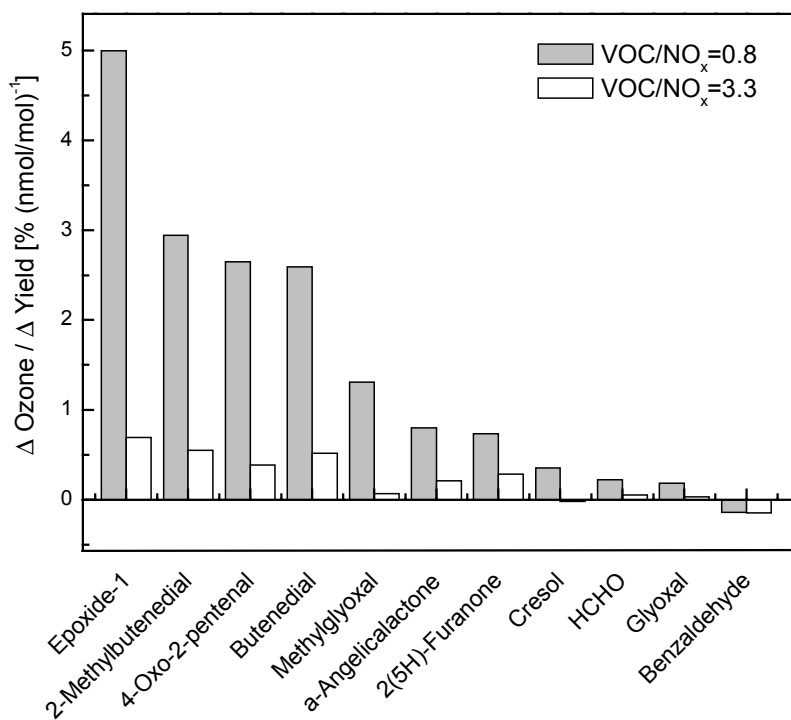
Fig. 9. Sensitivity of ozone to a change in the yields of intermediates calculated for the toluene-NO_x experiment 22/10/97 (initial VOC/NO_x = 3.3) and for a "model experiment" with the same initial toluene concentration but a VOC/NO_x ratio of 0.8.

either RO_2 is formed or HO_2 is released. This type of reaction could help to increase the RO_x production in the system and at the same time to reduce the NO_2 concentration and therewith the O_3 production.

A thorough understanding of the NO_y budget is a prerequisite to elucidate the reasons behind the model overestimate of ozone. Table 4 shows the simulated NO_y budget for the toluene experiment 22/10/97 at 15:00. Compounds are arranged into two groups: (1) NO_y species that can be measured with standard analytical equipment and (2) NO_y species for which quantification is a major analytical challenge. The contributions of HNO_3 and PAN to the NO_y budget are 31.1% and 25.5%, respectively. Including NO_2 and nitrocresol, compounds of the first group make up about 59.9% of total calculated NO_y. In the second group, nitroaromatics, mainly products of the cresol route, contribute 16.5%. A further 13.7% of the reactive NO_x is sequestered into PAN_y, which is represented in the model by 14 different compounds. Minor fractions of NO_x are converted to HNO_3 by wall reactions or go into the aerosol phase.

Owing to the low concentrations and the technical difficulties concerning the measurements of "problematic" NO_y compounds it is not feasible to obtain experimental closure in the NO_y budget by more than about 60%. However, experimental data on the most prominent species of each compound class is crucial to the identification of potential missing sinks of NO_x in the model.

5.2 O_3 sensitivities

An important parameter describing the tendency of a compound to produce O_3 is the O_3 sensitivity S_{O_3}, that describes the change in [O_3] caused by a change in a single model parameter. S_{O_3} was calculated by brute force, using the yields of intermediates as variables:

$$S_{O_3} = \frac{\Delta[O_3]}{\Delta[\text{yield of intermediate}]}.$$ (7)

For each run the yield of a single compound was changed by 20% and $\Delta[O_3]$ calculated as the difference in the integrals over the O_3 concentration time profiles of the run with the increased yield and the base run. The O_3 sensitivities were normalized and given as percentage change in the ozone concentration caused by a change of 1 nmol/mol in the yield of an intermediate. We have carried out sensitivity calculations for the 22/10/97 experiment with an initial VOC/NO_x ratio of 3.3 and for a "model experiment" with identical initial [toluene] but a VOC/NO_x ratio of 0.8.

Figure 9 shows that O_3 has the highest sensitivities to changes in the concentration of epoxide-1, conjugated γ-dicarbonyls and methylglyoxal. The sensitivities for cresol, formaldehyde and glyoxal are comparatively low and for benzaldehyde they are even negative, due to its low OH production rate and low tendency to convert NO into NO_2. There is a marked increase in the sensitivities of compounds, apart from benzaldehyde, at higher NO_x concentrations: on average, the sensitivities for epoxide-1 and conjugated γ-dicarbonyls are increased by a factor of 6. At a VOC/NO_x
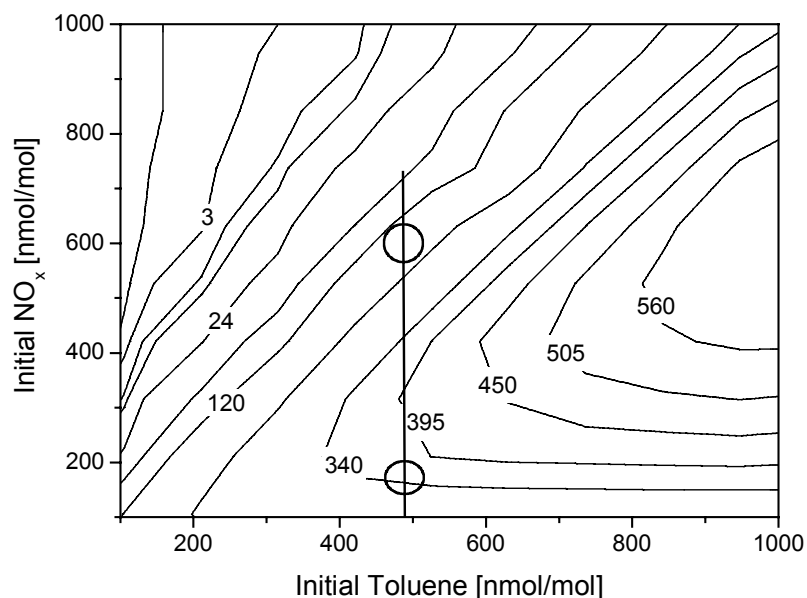
Fig. 10. Ozone isopleth plot for a toluene-NO_x system under chamber conditions. The maximum ozone concentration (in units of nmol/mol), during the course of an experiment is plotted as function of the initial NO_x and toluene concentrations. The circles indicate the conditions for the 22/10/97 experiment (VOC/NO_x ratio of 3.3) and the "model experiment" with a VOC/NO_x ratio of 0.8.

ratio of 0.8, the system is obviously VOC limited and the O_3 concentration is consequently much more sensitive to a change in the concentration of intermediates than under low NO_x conditions.

We have calculated an ozone isopleth plot for toluene-NO_x chamber experiments to check if the concept of VOC and NO_x limited regimes is applicable to these systems. As the VOC/NO_x ratio strongly increases during the course of an experiment (Fig. 3), we plotted the maximum ozone concentration as a function of the initial toluene and NO_x concentration (Fig. 10). The circles indicate the conditions for the 22/10/97 experiment (VOC/NO_x ratio of 3.3) and the "model experiment" with a VOC/NO_x ratio of 0.8. Depending on the initial conditions, the maximum ozone concentration in chamber experiments shows a behaviour analogous to that described in isopleth plots calculated for atmospheric conditions. At low NO_x concentrations the ozone production is NO_x limited and with increasing NO_x concentration the system passes a regime with maximum ozone productivity. At very high NO_x concentrations the system is VOC limited and the ozone concentration decreases with increasing NO_x concentrations. For the validation of atmospheric models, smog-chamber experiments with low NO_x concentrations that come close to atmospheric conditions are preferred. However, the NO_x dependency of the ozone sensitivity suggests that experiments at high NO_x levels, in the VOC limited region, are most suited to study the robustness of mechanisms with regards to the O_3 production.

To obtain more information on the impact of intermediates on the reactivity of the toluene system we have calculated the sensitivities of OH to a change in the yields of 25 first and second generation products. Figure 11 shows the correlation between the O_3 and OH sensitivities for the two

simulations with an initial VOC/NO_x ratio of 3.3 (22/10/97 experiment) and an initial VOC/NO_x ratio of 0.8. At the low VOC/NO_x ratio the sensitivities for OH and O_3 show a distinct correlation; the NO to NO_2 conversion clearly depends linearly on the OH yield from a compound. This implies that an over-prediction of the ozone concentration concurrent with an under-prediction of the reactivity in the toluene system at low VOC/NO_x (VOC-limited) is in contradiction with the calculated correlation between the sensitivities and would point to a photooxidation process that is not represented by any of the 25 compounds depicted in Fig. 11. At a VOC/NO_x ratio of 3.3 the OH and O_3 sensitivities no longer show a distinct correlation. In this NO_x limited regime the overall effect of a radical initiation process on the OH budget becomes also a function of the propensity of the radicals to terminate via peroxy-peroxy reaction. An over-prediction of the ozone concentration concurrent with an under-prediction of the OH production in the toluene system is no longer in contradiction with the results of the sensitivities analysis. As the ratio of OH to O_3 sensitivities of the intermediates varies over a wide range at low NO_x concentrations, an increase of yields for compounds with high OH but low O_3 sensitivities could bring simulations into agreement with experimental results. The sensitivity analysis shows that the toluene reaction system at high VOC/NO_x (NO_x-limited) ratios is far more complex and difficult to understand than under low VOC/NO_x (VOC-limited) conditions.

6 Conclusions and implications

In this study we have presented a number of modelling tools that help to improve our understanding of the shortcomings in detailed atmospheric mechanisms and that provide crucial
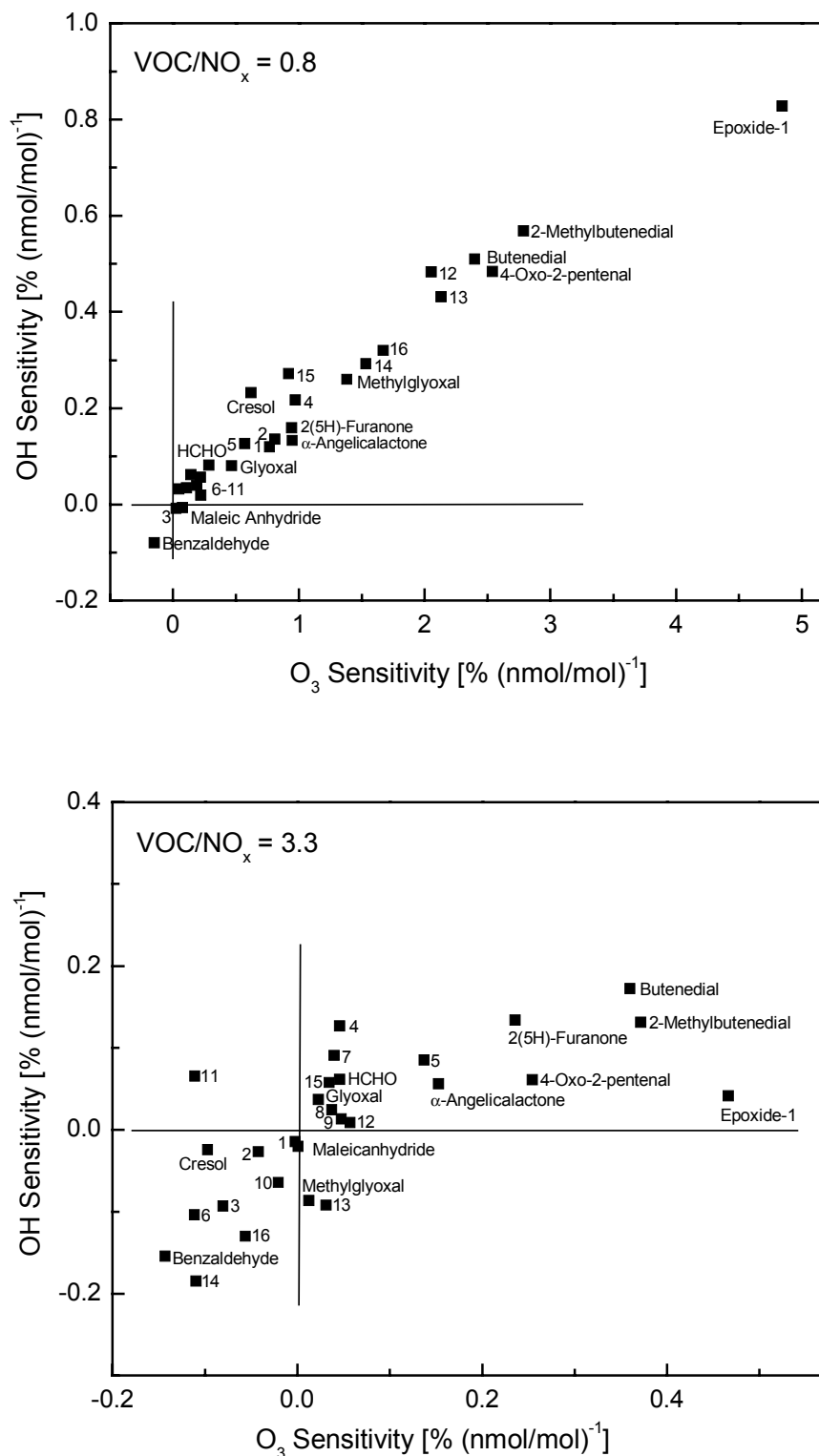
Fig. 11. Correlation between O_3 and OH sensitivities for first and second generation products in the toluene system. Correlation is shown for two different simulations with initial VOC/NO$_x$ ratios of 0.8 and 3.3 (22/10/97 experiment). Key to species: 1) 2,3-epoxybutandial; 2) methyl-1,4-benzoquinone; 3) acetaldehyde; 4) 4-hydroxy-3-methyl-cyclohexa-2,5-dienone; 5) 4-oxopent-2-enoic acid; 6) 2-hydroxy-3-oxo-butanal; 7) trioxopropane; 8) 4-hydroxy-dihydro-furan-2,3-dione; 9) 4-hydroxy-5-methyl-dihydro-furan-2,3-dione; 10) methyl-maleic anhydride; 11) 3-methyl-2,5-dioxo-hex-3-enedial; 12) 2-hydroxy-3,4-dioxo-pentanal; 13) 2,3,4-trioxopentanal; 14) 2,3-dioxobutanal; 15) glyoxylic acid; 16) 2,3-epoxy-4-hydroxy-5,6-dioxo-heptanal.

information for the design of future validation experiments. We have taken toluene for our case study. A comparison between simulation and smog-chamber data for a toluene-NO_x system revealed two major shortcomings in the mechanism: (1) a severe under-prediction of the radical production by about 44% and (2) an over-prediction of the ozone concentration by 55%. By calculating the RO_x budget of the system and O_3 and OH sensitivities we gained information on compounds and processes that govern the oxidation capacity in the toluene-NO_x system. Major findings are:

1. The RO_x budget calculations show that methylglyoxal, glyoxal, HCHO, epoxide-1, and conjugated γ-dicarbonyls are the dominant radical sources in the system. Radical production at the beginning of the experiments can only be explained by ring-opening intermediates, such as epoxide-1 or the conjugated γ-dicarbonyls, which have very high photolysis rates and are strong sources of new radicals. The photochemistry of this class of compounds is very poorly understood and the chemistry implemented in the toluene mechanism is very speculative. More experimental data on the co-products of glyoxal and methylglyoxal as well as the putative epoxide compounds are essential for a further improvement of the mechanism.

2. The over-prediction of ozone by the model is a more intricate problem as ozone production is linked to RO_x radical transformation. By calculating the NO_x budget it could be shown that, until O_3 reaches the maximum concentration, about two thirds of the NO to NO_2 conversion is linked to the production and oxidation of first generation products. The compounds which have the highest ozone sensitivities are epoxide-1 and the conjugated γ-dicarbonyls. To explain the ozone over-prediction we need to understand the interaction between radical production and the ozone creation potential of these compound classes. A general problem is that a reduction in NO to NO_2 conversion from a decrease in the peroxy radical formation will inevitably lead to less OH production and is therefore incompatible with the need to increase the oxidation capacity in the toluene system. We suggest two possible processes that might be responsible for the high reactivity in the experimental system and the concomitant comparatively low O_3 production: (i) processes that generate OH directly without or with only little NO to NO_2 conversion and (ii) NO_3 chemistry that sequesters reactive nitrogen oxides into stable NO_y compounds and at the same time produces HO_x radicals. As measurement techniques are available for only a few of the NO_x sinks, such as HNO_3, PAN-type compounds, nitroaromatics and alkylnitrates, closure of the NO_y budget is not feasible in the near future. However, measurements of a major representative of each compound class are essential to explain the O_3 over-prediction.

3. A sensitivity analysis has shown that the sensitivity of O_3 to a change in the concentration of intermediates is highest at high NO_x concentration. Thus, validation experiments in the VOC limited regime are particularly suited to test mechanisms on major shortcomings in their O_3 productivity. At low NO_x concentrations the O_3 and OH sensitivities no longer show a distinct correlation and photochemical processes become much more complex as peroxy-peroxy termination gains importance and becomes an additional parameter influencing the OH and O_3 production potential of a compound.

For a further improvement of the toluene mechanism, quantification of the co-products (conjugated γ-dicarbonyls) of glyoxal and methylglyoxal and the major intermediates in the putative epoxide route will be crucial. Furthermore, the sub-mechanisms describing the photochemistry of those compounds that have, according to our current knowledge, the highest impact on OH and O_3 formation should be validated against single-component experiments. A crucial question is how much NO_x is sequestered into nitro-organic compounds. With more information on the photochemistry of intermediates and the NO_y budget emerging, it will be possible to gradually improve the toluene mechanism so that OH as well as O_3 can be reliably predicted over a broad range of NO_x concentrations, from highly polluted to remote conditions, as is essential for atmospheric models.

References

Atkinson, R., Carter, W. P. L., Darnall, K. R., Winer, A. M., and Pitts, Jr., J. N.: A smog-chamber and modelling study of the gas phase NO_x-air photooxidation of toluene and the cresols, Int. J. Chem. Kinet., 12, 779–834, 1980.

Atkinson, R.: A structure-activity relationship for the estimation of rate constants for the gas-phase reactions of OH radicals with organic compounds, Int. J. Chem. Kinetics., 19, 799–828, 1987.

Atkinson, R.: Gas-phase tropospheric chemistry of organic compounds, J. Phys. Ref. Data, Monograph, 2, 47–59, 1992.

Bartolotti, L. J. and Edney, E. O.: Density functional theory derived intermediates from the OH initiated atmospheric oxidation of toluene, Chem. Phys. Lett., 245, 119–122, 1995.

Berndt, T., Böge, O., and Herrmann, H.: On the formation of benzene oxide / oxepin in the gas-phase of OH radicals with benzene, Chem. Phys. Lett., 314, 435–442, 1999.

Bierbach, A., Barnes, I., Becker, K. H., and Wiesen, E.: Atmospheric chemistry of unsaturated carbonyls: Butenedial, 4-oxo-2-pentenal, 3-hexene-2,5-dione, maleic anhydride, 3H-furan-2-one, and 5-methyl-3H-furan-2-one, Environ. Sci. Technol., 28, 715–729, 1994.

Bohn, B. and Zetzsch, C.: Gas-phase reaction of the OH-benzene adduct with O$_2$: Reversibility and secondary formation of HO$_2$, Phys. Chem. Chem. Phys., 1, 5097–5107, 1999.

Bohn, B.: Formation of peroxy radicals from OH-toluene adducts and O$_2$, J. Phys. Chem. A, 105, 6092–6101, 2001.

Derwent, R. G., Jenkin, M. E., and Saunders, S. M.: Photochemical ozone creation potentials for a large number of reactive hydrocarbons under European conditions, Atmos. Environ., 30, 181–199, 1996.

Derwent, R. G., Jenkin, M. E., Saunders, S. M., and Pilling, M. J.: Photochemical ozone creation potentials for organic compounds in northwest Europe calculated with a Master Chemical Mechanism, Atmos. Environ., 32, 2429–2441, 1998.

Ghigo, G. and Tonachini, G.: From benzene to muconaldehyde: Theoretical mechanistic investigation on some tropospheric oxidation channels., J. Am. Chem. Soc., 121, 8366–8372, 1999.

Jang, M. and Kamens, R. M.: Characterization of secondary aerosol from the photooxidation of toluene in the presence of NO$_x$ and 1-propene, Environ. Sci. Technol., 35, 3626–3639, 2001.

Jenkin, M. E., Hayman, G. D., Wallington, T. J., Hurley, M. D., Ball, J. C., Nielsen, O. J., and Ellermann, T.: Kinetic and mechanistic study of the self reaction of CH$_3$OCH$_2$O$_2$ radicals at room temperature, J. Phys. Chem., 97, 11 712–11 723, 1993.

Jenkin, M. E. and Clemitshaw, K. C.: Ozone and other secondary photochemical pollutants: chemical processes governing their formation in the planetary boundary layer, Atmos. Environ., 34, 2499–2527, 2000.

Jenkin, M. E., Saunders, S. M., Wagner, V., and Pilling, M.: Protocol for the development of the Master Chemical Mechanism, MCM v3 (Part B): tropospheric degradation of aromatic volatile organic compounds, Atmos. Chem. Phys. Discuss., 2, 1905–1938, 2002.

Klotz, B., Barnes, I., Becker, K. H., and Golding, B. T.: Atmospheric chemistry of benzene oxide/oxepin, J. Chem. Soc., Faraday Trans., 93, 1507–1516, 1997.

Klotz, B., Sørensen, S., Barnes, I., Becker, K. H., Etzkorn, T., Volkamer, R., Platt, U., Wirtz, K., and Montserrat, M.-R.: Atmospheric oxidation of toluene in a large-volume outdoor photoreactor: In situ determination of ring-retaining product yields, J. Phys. Chem., 102, 10 289–10 299, 1998.

Klotz, B., Barnes, I., Golding, B. T., and Becker, K.-H.: Atmospheric chemistry of toluene-1,2-oxide/2-methyloxepin, Phys. Chem. Chem. Phys., 2, 227–235, 2000.

Kwok, E. and Atkinson, R.: Estimation of hydroxyl radical rate constants for gas-phase organic compounds using a structure-reactivity relationship: an update, Atmos. Environ., 29, 1685–1695, 1995.

Liang, J. and Jacobson, M. Z.: Comparison of a 4000-reaction chemical mechanism with the carbon bond IV and an adjusted carbon bond IV-EX mechanism using SMVGEAR II, Atmos. Environ., 34, 3015–3026, 2000.

Liu, X. Y., Jeffries, H. E., and Sexton, K. G.: Atmospheric photochemical degradation of 1,4-unsaturated dicarbonyls, Environ. Sci. Technol., 33, 4212–4220, 1999.

Motta, F., Ghigo, G., and Tonachini, G.: Oxidative degradation of benzene in the troposphere. Theoretical mechanistic study of the formation of unsaturated dialdehydes and dialdehyde epoxides, J. Phys. Chem. A, 106, 4411–4422, 2002.

Olariu, R. I., Klotz, B., Barnes, I., Becker, K. H., and Mocanu, R.: FT-IR study of the ring-retaining products from the reaction of OH radicals with phenol, o-, m-, and p-cresol, Atmos. Environ., 36, 3685–3697, 2002.

Saunders, S. M., Jenkin, M. E., Derwent, R. G., Pilling, M. J.: Protocol for the development of the Master Chemical Mechanism, MCM v3 (Part A): tropospheric degradation of non-aromatic volatile organic compounds, Atmos. Chem. Phys. Discuss., 2, 1847–1903, 2002.

Seuwen, R. and Warneck, P.: Oxidation of toluene in NO$_x$ free air: Product distribution and mechanism, Int. J. Chem. Kinet., 28, 315–332, 1996.

Smith, D. F., McIver, C. D., and Kleindienst, T. E.: Primary product distribution from the reaction of hydroxyl radicals with toluene at ppb NO$_x$ mixing ratios, J. Atmos. Chem., 30, 209–228, 1998.

Sørensen, S., Barnes, I., and Becker, K. H.: Photolysis of unsaturated 1,4-dicarbonyls under atmospheric conditions in the European photoreactor (EUPHORE), Environ. Sci. and Poll. Res., 5, 159, 1998.

Volkamer, R., Platt, U., and Wirtz, K.: Primary and secondary glyoxal formation from aromatics: Experimental evidence for the bicycloalkyl-radical pathway from benzene, toluene, and p-xylene, J. Phys. Chem. A, 105, 7865–7874, 2001.

Volkamer, R., Klotz, B., Barnes, I., Imamura, T., Wirtz, K., Washida, N., Becker, K. H., and Platt, U.: OH-initiated oxidation of benzene: Part 1. Phenol formation under atmospheric conditions, Phys. Chem. Chem. Phys., 4, 1598–1610, 2002.

Wayne, R. P., Barnes, I., Biggs, P., Burrows, J. P., Canosa-Mas, C. E., Hjorth, J., Le Bras, G., Moortgat, G. K., Perner, D., Poulet, G., Restelli, G., and Sidebottom, H.: The nitrate radical: Physics, chemistry, and the atmosphere, Atmos. Environ., 25A, 1–203, 1991.

Yu, J. and Jeffries, H.: Atmospheric photooxidation of alkylbenzenes – II Evidence of formation of epoxide intermediates, Atmos. Environ., 31, 2281–2287, 1997.

Yu, J., Jeffries, H., and Sexton, K. G.: Atmospheric photooxidation of alkylbenzenes – I. Carbonyl product analyses, Atmos. Environ., 31, 2261–2280, 1997.